TIME SCALE ANALYSIS AND SYNTHESIS FOR MODEL PREDICTIVE CONTROL

Yan Zhang *
Nanjing University of Science and Technology
Nanjing, China
zhanyan@isu.edu

Hoa Nguyen
Idaho State University
Pocatello, Idaho, USA
nguyhoa@isu.edu

D. Subbaram Naidu
Idaho State University
Pocatello, Idaho, USA
naiduds@isu.edu

Yun Zou
Nanjing University of Science and Technology
Nanjing, China
zouyun@vip.163.com

Chenxiao Cai
Nanjing University of Science and Technology
Nanjing, China
ccx5281@vip.163.com

Abstract: This paper presents time scale analysis and synthesis (control) methodology for Model Predictive Control (MPC). In this method, a higher-order plant with a two-time (slow and fast) scale character is analyzed (decoupled) into low-order slow and fast subsystems and sub-augmented systems. Then slow and fast subcontrollers based on MPC method are synthesized (designed) separately and a composite MPC is obtained. The methodology is illustrated for a high-order Wind Energy Conversion Systems (WECS) with Permanent Magnet Synchronous Generators (PMSG). The results show that the performance of the system with composite MPC is very close to that of the MPC of the original high-order system showing the superiority of the proposed method in terms of separation of dynamics, simplicity in designing model predictive controllers and reduced computational effort.

Key–Words: Singular perturbations, wind energy conversion systems, time scales, model predictive control, order reduction

1 Introduction

In physical world, modeling of many systems calls for high-order and ill-conditioned dynamic equations because of the presence of some parasitic parameters such as small time constants, resistances, inductances, capacitances, moments of inertia, and Reynolds number. The high dimensionality and ill-conditioned numerical issues in the system, attributed to the simultaneous occurrence of slow and fast phenomena, give rise to time scales [1]. The curse of dimensionality coupled with ill-conditioned dynamics poses formidable computational complexities for the analysis and design of multiple time-scale systems.

The methodology of singular perturbations and time-scales (SPaTS) has obtained intensively attention during the past three decades because of its dimensional reduction and stiffness relief [1, 2].

Wind energy has been growing rapidly during the last two decades [3, 4, 5, 6] and advances in technology have enabled wind energy conversion systems (WECSs) to reach mega-watt (MW) ranges of power [7, 8]. Such systems with both mechanical and electrical components can be viewed as singularly perturbed or two-time scale systems [3, 9, 10].

Model Predictive Control (MPC) is a form of control in which the current control action is obtained by solving on-line a finite horizon open-loop optimal control problem, using the current state of the plant as the initial state at each sampling instant. The optimization yields an optimal control sequence and the first control in this sequence is applied to the plant [11]. It has received on-going interest from researchers in both the industrial and academic communities because of its ability to handle both soft constraints and hard constraints in a multivariable control framework and the ability to perform on-line process optimization [12, 13, 14, 17]. MPC is used to design a composite controller for nonlinear singularly perturbed systems in [15]. Reference [16] studies the MPC control for linear two-time-scale systems with and without time delay.

In this study, we present time scale analysis and synthesis (control) methodology for continuous-time Model Predictive Control (MPC). In this method, a

*Presently Visiting Research Scholar, Measurement and Control Engineering Research Center, Idaho State University, Pocatello, ID, USA

higher-order plant with a two-time-scale (slow and fast) character is analyzed (decoupled) into low-order slow and fast subsystems. Model predictive controllers are designed for two subsystems separately based on augmented models. Then the discrete-time Model Predictive Control is also introduced. Applying this method to WECS in both continuous-time and discrete-time region, the results show that the performance of the system with continuous-time composite MPC is very close to that of the continuous-time MPC of the original high-order system showing the superiority of the proposed method in terms of separation of dynamics, simplicity in designing model predictive controllers and reduced computational effort.

The remainder of this paper is organized as follows. In section II, modeling of the WECS is presented followed by time-scale analysis for decoupling the original high-order system into low-order slow and fast subsystems. Section IV describes the continuous-time MPC method to design controllers for slow and fast subsystems and discrete-time MPC method. The simulation results are given in Section V. Finally Section VI discusses the conclusion of this work.

2 Modeling

2.1 Nonlinear Model

In general, a WECS is a system that converts wind power into electrical power. The devices of a WECS can be grouped as functional blocks with respect to power flow as shown in Fig. 1[3]. The wind power is converted into mechanical power (rotations) in the aerodynamics block, and this mechanical power (rotations) is transmitted to the generator block by the drive train block. In the generator block, the mechanical power is transformed into electrical power.

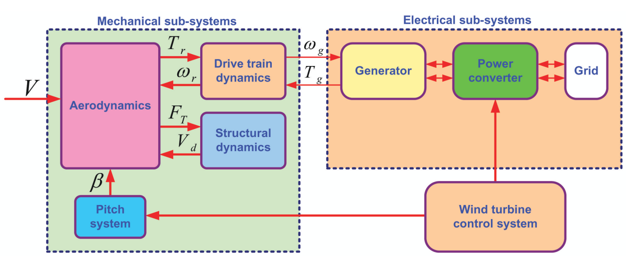

Figure 1: WECS Block Diagram[3]

For the control purpose, only aerodynamics, drive train dynamics, and generator dynamics are taken into account. The aerodynamics takes the wind speed V and wind rotor speed ω_r as inputs. The output is given in terms of aerodynamics torque T_r as follows:

$$T_r = \frac{1}{2}\rho\pi R^3 C_Q(\lambda,\beta)V^2, \tag{1}$$

where ρ is the air density, R is the radius of the wind rotor plane, C_Q is the torque coefficient given as a function of the pitch angle β and the tip-speed ratio λ, where λ is defined as

$$\lambda = \frac{\omega_r R}{V}, \tag{2}$$

where ω_r is the wind rotor speed. The torque coefficient C_Q can be approximated by a polynomial of λ:

$$\begin{aligned} C_Q(\lambda) &= a_0 + a_1\lambda + a_2\lambda^2 + a_3\lambda^3 + a_4\lambda^4 \\ &\quad + a_5\lambda^5 + a_6\lambda^6. \end{aligned} \tag{3}$$

The drive train block consists of a low-speed shaft and a high-speed shaft connected to each other through a gearbox which increases the rotational speed. The drive train can be represented by a rigid or flexible model. In this study, a flexible drive train is used which has the model:

$$\dot{\omega}_r = -\frac{i}{\eta J_r}T_H + \frac{1}{J_r}T_r \tag{4}$$

$$\dot{\omega}_g = \frac{1}{J_g}T_H - \frac{1}{J_g}T_g \tag{5}$$

$$\begin{aligned} \dot{T}_H &= iK_g\omega_r - K_g\omega_g - B_g\left(\frac{1}{J_g} + \frac{i^2}{\eta J_r}\right)T_H \\ &\quad + \frac{iB_g}{J_r}T_r + \frac{B_g}{J_g}T_g \end{aligned} \tag{6}$$

where ω_g is the generator speed, T_H is the internal torque, J_r is the wind rotor inertia, J_g is the generator inertia, K_g is the stiffness coefficient of the high-speed shaft, B_g is the damping coefficient of the high-speed shaft (the generator shaft), i is the gearbox ratio, and η is the gearbox efficiency.

Essentially, asynchronous and synchronous generators are two primary types of generator which have been used in WECSs. Three popular generators are Squirrel Cage Induction Generator (SCIG), Doubly Fed Induction Generator (DFIG), and Permanent Magnet Synchronous Generator (PMSG) [9, 18]. This study is focused on the PMSG which has the model in (d,q) axes as follows:

$$\dot{i}_d = -\frac{R_s}{L_d}i_d + \frac{pL_q}{L_d}i_q\omega_g - \frac{1}{L_d}u_d, \tag{7}$$

$$\dot{i}_q = -\frac{R_s}{L_q}i_q - \frac{p}{L_q}(L_d i_d - \phi_m)\omega_g - \frac{1}{L_q}u_q, \tag{8}$$

$$T_g = p\phi_m i_q, \tag{9}$$

where i_d, L_d, u_d and i_q, L_q, u_q are the d and q components of the stator current, inductance, voltage, respectively; R_s is the stator resistance; P is the number of pole pairs, ϕ_m is the flux.

The complete nonlinear model of a PMSG-based WECS is obtained by combining (4)-(8).

2.2 Linear Model

Choosing an operating point with $\bar{x} = [\bar{\omega}_r \, \bar{\omega}_g \, \bar{T}_H \, \bar{i}_d \, \bar{i}_q]^T$ and $\bar{u} = [\bar{u}_d \, \bar{u}_q \, \bar{V}]^T$, the linearized model is obtained as follows

$$\dot{\delta}_x = A\delta_x + B\delta_u, \tag{10}$$

where $\delta_x = x - \bar{x}$ and $\delta_u = u - \bar{u}$ are variations of variables in the neighborhood of the operating point. The system and control matrices are given as:

$$A = \begin{bmatrix} \frac{1}{2J_r\bar{\omega}_r}\rho\pi R^3 C_Q(\bar{\lambda})\gamma\bar{V}^2 & 0 & -\frac{i}{\eta J_r} & 0 & 0 \\ 0 & 0 & \frac{1}{J_g} & 0 & -\frac{p\phi_m}{J_g} \\ iK_g + \frac{iB_g}{2J_r\bar{\omega}_r}\rho\pi R^3 C_Q(\bar{\lambda})\gamma\bar{V}^2 & -K_g & -B_g\left(\frac{1}{J_g} + \frac{i^2}{\eta J_r}\right) & 0 & \frac{B_g p\phi_m}{J_g} \\ 0 & \frac{pL_q}{L_d}\bar{i}_q & 0 & -\frac{R_s}{L_d} & \frac{pL_q\bar{\omega}_g}{L_d} \\ 0 & -\frac{p}{L_q}\left(L_d\bar{i}_d - \phi_m\right) & 0 & -\frac{pL_d\bar{\omega}_g}{L_q} & -\frac{R_s}{L_d} \end{bmatrix}, \tag{11}$$

$$B = \begin{bmatrix} 0 & 0 & \frac{2-\gamma}{2J_r}\rho\pi R^3 C_Q(\bar{\lambda})\bar{V} \\ 0 & 0 & 0 \\ 0 & 0 & \frac{2-\gamma}{2J_r}iB_g\rho\pi R^3 C_Q(\bar{\lambda})\bar{V} \\ -\frac{1}{L_d} & 0 & 0 \\ 0 & -\frac{1}{L_q} & 0 \end{bmatrix}, \tag{12}$$

where $\gamma = \frac{\bar{\lambda}C_Q'(\bar{\lambda})}{C_Q(\bar{\lambda})}, \lambda = \frac{\omega_r R}{V}, C_Q(\lambda) = a_0 + a_1\lambda + a_2\lambda^2 + a_3\lambda^3 + a_4\lambda^4 + a_5\lambda^5 + a_6\lambda^6$.

3 Time Scale Analysis

3.1 Two-time-scale Property of the PMSG-based WECS

Assume $V = 10\,m/s$, a linear model is derived. The system and control matrices of the linear model are obtained as

$$A = \begin{bmatrix} -1.0133 & 0 & -2.0833 & 0 & 0 \\ 0 & 0 & 4.5455 & 0 & -5.9755 \\ 448.1760 & -75.0000 & -5.1136 & 0 & 1.7926 \\ 0 & 10.5141 & 0 & -79.4033 & 441.7308 \\ 0 & 18.2715 & 0 & -441.7308 & -79.4033 \end{bmatrix}, \tag{13}$$

$$B = \begin{bmatrix} 0 & 0 & 18.3058 \\ 0 & 0 & 0 \\ 0 & 0 & 32.9504 \\ -24.0616 & 0 & 0 \\ 0 & -24.0616 & 0 \end{bmatrix}. \tag{14}$$

This linear system has five eigenvalues $P_1 = -0.2$, $P_2 = -2.92 + j35.63$, $P_3 = -2.92 - j35.63$, $P_4 = -79.45 + j441.86$, $P_5 = -79.45 - j441.86$.

The first three eigenvalues P_1, P_2, P_3 are close to the origin which characterizes the slow response for the system. The other two eigenvalues P_4 and P_5 are far from the origin characterizing the fast dynamics of the system.

The distance between these two eigenvalue clusters is computed by dividing the largest absolute value of the slow group by the smallest absolute value of the fast group [10]. In this case the computed distance, called the small parameter, is $\varepsilon = 0.036$. A system is said to have a two-time-scale property if $\varepsilon \ll 1$ [10], thereby it is concluded that the PMSG-based WECS has a two-time-scale property.

3.2 Two-Time-Scale System Decoupling

In this section, the system decoupling procedure is briefly described [10, 19]. Consider a general two-time-scale linear system

$$\dot{x}_1 = A_1x_1 + A_2x_2 + B_1u, \tag{15}$$
$$\dot{x}_2 = A_3x_1 + A_4x_2 + B_2u, \tag{16}$$

where x_1 and x_2 are $m-$ and $n-$ dimensional slow and fast state vectors, respectively, u is an $r-$dimensional control vector, $A_i (i = 1, 2, 3, 4)$, are system matrices with appropriate dimensions, B_1, B_2 are control matrices with appropriate dimensions. The system (15)-(16) can be decoupled into a slow subsystem and a fast subsystem using the well-known Chang transformation [19]. This transformation includes two phases. The first phase transforms the system (15)-(16) into the form

$$\begin{bmatrix} \dot{x}_1 \\ \dot{x}_f \end{bmatrix} = \begin{bmatrix} A_s & A_2 \\ 0 & A_f \end{bmatrix} \begin{bmatrix} x_1 \\ x_f \end{bmatrix} + \begin{bmatrix} B_1 \\ B_f \end{bmatrix} u \quad (17)$$

by using the change of variable $x_f = x_2 + Lx_1$ and choosing the matrix L $(n \times m)$ such that

$$LA_1 - A_4L - LA_2L + A_3 = 0, \quad (18)$$

where

$$\begin{aligned} A_s &= A_1 - A_2L, & (19)\\ A_f &= A_4 + LA_2, & (20)\\ B_f &= B_2 + LB_1. & (21) \end{aligned}$$

The second phase continues to transform the system (17) into the form

$$\begin{bmatrix} \dot{x}_s \\ \dot{x}_f \end{bmatrix} = \begin{bmatrix} A_s & 0 \\ 0 & A_f \end{bmatrix} \begin{bmatrix} x_s \\ x_f \end{bmatrix} + \begin{bmatrix} B_s \\ B_f \end{bmatrix} u \quad (22)$$

by using the change of variable $x_s = x_1 - Hx_f$ and choosing the matrix H $(m \times n)$ such that

$$A_sH - HA_f + A_2 = 0, \quad (23)$$

where

$$B_s = B_1 - HLB_1 - HB_2. \quad (24)$$

Note that the system (22) includes two independent subsystems represented by (A_s, B_s) and (A_f, B_f), where A_s, A_f, B_f, and B_s are given in (19), (20), (21), and (24), respectively.

3.3 Numerical Solutions

The decoupled subsystems can be obtained if there exist two matrices L and H which satisfy (18) and (23), respectively. Analytical solutions for those equations haven't been found yet, therefore approximate solutions are obtained numerically. One efficient numerical algorithm is the Newton algorithm [3, 20].

Applying Newton algorithm to the linear PMSG-based WECS (13) and (14), The results show that the Newton algorithm was convergent with solutions L and H given as

$$L = \begin{bmatrix} 0.0005 & -0.0443 & -0.0001 \\ 0.0000 & 0.0158 & -0.0005 \end{bmatrix}, \quad (25)$$

$$H = \begin{bmatrix} 0.0004 & 0.0003 \\ -0.3159 & 0.0561 \\ 0.0771 & -0.0670 \end{bmatrix}. \quad (26)$$

The slow subsystem is obtained as

$$\underbrace{\begin{bmatrix} \dot{\delta}_{\omega_r} \\ \dot{\delta}_{\omega_g} \\ \dot{\delta}_{T_H} \end{bmatrix}}_{\dot{x}_s} = A_s \underbrace{\begin{bmatrix} \delta_{\omega_r} \\ \delta_{\omega_g} \\ \delta_{T_H} \end{bmatrix}}_{x_s} + B_s \underbrace{\begin{bmatrix} \delta_{u_d} \\ \delta_{u_q} \\ \delta_V \end{bmatrix}}_{u_s}, \quad (27)$$

where

$$A_s = \begin{bmatrix} -1.0133 & 0 & -2.0833 \\ 0 & 0.0947 & 4.5426 \\ 448.1760 & -75.0284 & -5.1128 \end{bmatrix} \quad (28)$$

$$B_s = \begin{bmatrix} 0.0089 & 0.0072 & 0 \\ -7.6008 & 1.3488 & 0 \\ 1.8552 & -1.6120 & 0 \end{bmatrix}, \quad (29)$$

And the fast subsystem is obtained as

$$\underbrace{\begin{bmatrix} \dot{\delta}_{i_d} \\ \dot{\delta}_{i_q} \end{bmatrix}}_{\dot{x}_f} = A_f \underbrace{\begin{bmatrix} \delta_{i_d} \\ \delta_{i_q} \end{bmatrix}}_{x_f} + B_f \underbrace{\begin{bmatrix} \delta_{u_d} \\ \delta_{u_q} \\ \delta_V \end{bmatrix}}_{u_f}, \quad (30)$$

where

$$A_f = \begin{bmatrix} -79.4033 & 441.9953 \\ -441.7308 & -79.4988 \end{bmatrix}, \quad (31)$$

$$B_f = \begin{bmatrix} -24.0616 & 0 & 0 \\ 0 & -24.0616 & 0 \end{bmatrix}. \quad (32)$$

The slow subsystem has three eigenvalues $P_{s_1} = -0.2007$, $P_{s_2} = -2.9154 + j35.6295$, $P_{s_3} = -2.9154 - j35.6295$ which are almost the same as the slow eigenvalues of the original system (13) and (14).

Similarly, the fast subsystem also has two eigenvalues $P_{f_1} = -79.45 + j441.86$, $P_{f_2} = -79.45 + j441.86$ which are also almost the same as the fast eigenvalues of the system (13) and (14).

Therefore, the decoupling was reliable.

4 Model Predictive Control for Two-Time-Scale PMSG-based WECS

4.1 Continuous-Time Model Predictive Control

The two-time-scale PMSG-based WECS is now decoupled into two independent subsystems, the control design is therefore independent for each subsystem. Based on two subsystems, augmented models are derived and two continuous model predictive controllers are designed separately for fast and slow subsystems.

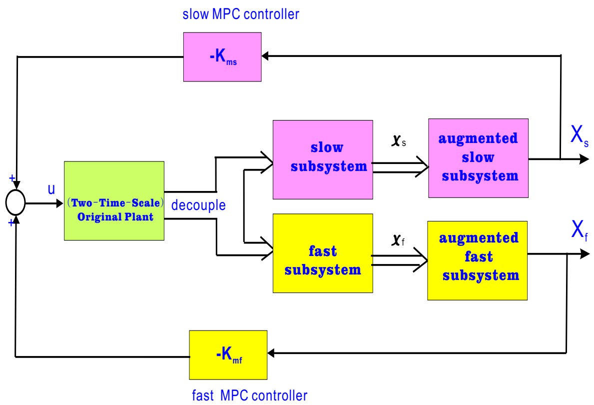

Figure 2: Two-Time-scale Decoupling of MPC

The final control which is fed to the original system will be the composite of the controls from two subsystems as indicated in Fig. 2.

MPC refers to a class of computer control algorithms that utilize an explicit process model to predict the future response of a plant. At each control interval an MPC algorithm attempts to optimize future plant behavior by computing a sequence of future manipulated variable adjustments. The first input in the optimal sequence is then sent into the plant and the entire calculation is repeated at subsequent control intervals [12].

Fig. 3 is the closed-loop block diagram of continuous-time model predictive control method..

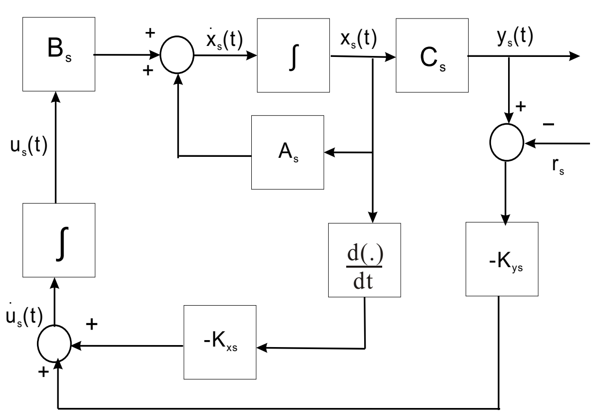

Figure 3: Block diagram of Continuous-Time MPC of Slow Subsystem.

In this section, we consider the slow subsystem as an example to show the process of designing a continuous-time model predictive controller. For the fast subsystem and the original system, we can design the continuous-time model predictive controllers using the same method.

Now let us consider the slow subsystem as given below:

$$\begin{aligned} \dot{x}_s &= A_s x_s + B_s u_s && (33) \\ y_s &= C_s x_s && (34) \end{aligned}$$

with the cost function

$$\begin{aligned} J_s &= \int_0^{T_p} (X_s'(t_i+\tau|t_i) Q_s X_s(t_i+\tau|t_i) \\ &\quad + \dot{u}_s'(\tau) R_s \dot{u}_s(\tau)) d\tau && (35) \end{aligned}$$

where T_p is the prediction horizon, $X_s(t_i+\tau)$ is the state of augmented model as below:

$$X_s(t) = \begin{bmatrix} \dot{x}_s(t) \\ y_s(t) - r_s(t) \end{bmatrix} \quad (36)$$

$$\begin{aligned} \dot{X}_s(t) &= \begin{bmatrix} \ddot{x}_s(t) \\ \dot{y}_s(t) - \dot{r}_s(t) \end{bmatrix} \\ &= \begin{bmatrix} A_s & 0 \\ C_s & 0 \end{bmatrix} \begin{bmatrix} \dot{x}_s(t) \\ y_s(t) - r_s(t) \end{bmatrix} + \\ &\quad \begin{bmatrix} B_s \\ 0 \end{bmatrix} \dot{u}_s(t) \\ &\triangleq A_p X_s(t) + B_p \dot{u}_s(t) && (37) \end{aligned}$$

where

$$A_p = \begin{bmatrix} A_s & 0 \\ C_s & 0 \end{bmatrix}, \quad B_p = \begin{bmatrix} B_s \\ 0 \end{bmatrix} \quad (38)$$

In order to follow the set-point signal, the control signal needs to converge to a non-zero constant that is related to the steady-state gain of the plant and the magnitude of the set-point change. Therefore, instead of modeling the control signal, the continuous-time predictive control design will target the derivative of the control signal, $\dot{u}(t)$, which will satisfy the property

$$\int_0^{\infty} \dot{u}_s^2(t) dt < \infty \quad (39)$$

A set of Laguerre functions $L(\tau)$ is used as orthonormal basis functions [12].

According to [12], the derivative of the control signal can be described as:

$$\dot{u}_s(\tau) \approx \sum_{i=1}^{N} C_i l_i(\tau) = L'(\tau)\eta \quad (40)$$

Where $\eta = [c_1 \quad c_2 \quad \cdots \quad c_N]'$ is the coefficient vector.

Let t_i be the current time, and assume the state variable $X_s(t_i)$ is available. Then at the future time

τ, $\tau > 0$, the predicted state variable $X_s(t_i + \tau|t_i)$ is described by the following equation:

$$X_s(t_i + \tau|t_i) = e^{A_p\tau}X_s(t_i) + \int_0^{\tau} e^{A_p(\tau-\gamma)}B_s\dot{u}_s(\gamma)d\gamma \quad (41)$$

According to (40), we have $\dot{u}_{si}(\tau) = L_i'(\tau)\eta_i$, then the predicted future state $X_s(t_i + \tau|t_i)$ at time τ is:

$$X_s(t_i + \tau|t_i) = e^{A_p\tau}X_s(t_i) + \int_0^{\tau} e^{A_p(\tau-\gamma)}[B_{s1}L_1'(\gamma)\cdots B_{sm}L_m'(\gamma)]d\gamma\eta \quad (42)$$

written as

$$X(t_i + \tau|t_i) = e^{A_p\tau}X(t_i) + \Phi'(\tau)\eta \quad (43)$$

where $\Phi'(\tau)$ is the convolution integral with

$$\Phi'(\tau) = \int_0^{\tau} e^{A_s(\tau-\gamma)}[B_{s1}L_1'(\gamma)\cdots B_{sm}L_m'(\gamma)]d\gamma$$

We assume that R_s is a diagonal matrix with

$$R_s = diag\{r_k\} \quad (44)$$

where $k = 1, 2, \cdots, m$. Then the second term in the cost function (35) is

$$\int_0^{T_p} \dot{u}_s'(\tau)R\dot{u}_s(\tau)d\tau = \sum_{k=1}^{m} r_k \int_0^{T_p} \dot{u}_{sk}^2(\tau) \quad (45)$$

The prediction horizon is selected to be larger than then the time for which the control signal is effective, thus

$$\int_0^{T_p} \dot{u}_{sk}'(\tau)\dot{u}_{sk}(\tau)d\tau \approx \int_0^{\infty} \eta_k' L_k(\tau)L_k'(\tau)\eta_k d\tau = \eta_k'\eta_k \quad (46)$$

Since $\int_0^{\infty} L_k(\tau)L_k'(\tau)d\tau$ is the identity matrix with dimension equal to the number of Laguerre coefficients for the kth input. The cost function J_s is then equivalently given by

$$\int_0^{T_p} (X_s'(t_i + \tau|t_i)Q_sX_s(t_i + \tau|t_i) + \eta' R_L\eta \quad (47)$$

where R_L is a block diagonal matrix with the kth block being R_k, and $R_k = r_k I_{N_k \times N_k}$. Using (43) in (47), we get J_s as

$$J_s = \int_0^{T_p} (e^{A_p\tau}X_s(t_i) + \Phi'(\tau)\eta)'Q_s (e^{A_p\tau}X(t_i)\Phi'(\tau)\eta)d\tau + \eta' R_L\eta \quad (48)$$

which is a quadratic function of η

$$\begin{aligned} J_s &= \eta' \left\{ \int_0^{T_p} \Phi(\tau)Q_s\Phi'(\tau)d\tau + R_L \right\} \eta \quad (49) \\ &+2\eta' \left\{ \int_0^{T_p} \Phi(\tau)Q_s e^{A_p\tau}d\tau \right\} X_s(t_i) \\ &+X_s'(t_i) \left\{ \int_0^{T_p} e^{A_p'\tau}Q_s e^{A_p\tau}d\tau \right\} X_s(t_i) \end{aligned}$$

For notational simplicity, we define

$$\Omega = \int_0^{T_p} \Phi(\tau)Q_s\Phi'(\tau)d\tau + R_L \quad (50)$$

$$\Psi = \int_0^{T_p} \Phi(\tau)Q_s e^{A_p\tau}d\tau \quad (51)$$

Completing the square of (49) leads to

$$\begin{aligned} J_s &= [\eta + \Omega^{-1}\Psi X_s(t_i)]'\Omega[\eta + \Omega^{-1}\Psi X_s(t_i)] \\ &+X_s'(t_i) \int_0^{T_p} e^{A_p'\tau}Q_s e^{A_p\tau}d\tau X_s(t_i) \\ &-X_s'(t_i)\Psi'\Omega^{-1}\Psi X_s(t_i) \end{aligned}$$

Since the last two terms are independent of η , the optimal η that minimizes J is:

$$\eta = -\Omega^{-1}\Psi X_s(t_i) \quad (52)$$

and the minimum of the cost function J_{smin} is:

$$X_s'(t_i) \left[\int_0^{T_p} e^{A_p'\tau}Q_s e^{A_p\tau}d\tau - \Psi'\Omega^{-1}\Psi \right] X_s(t_i) \quad (53)$$

So feedback gain matrix K_{ms} is as below:

$$\begin{aligned} K_{ms} &= \begin{bmatrix} L_1'(\tau) & o_2 & \cdots & o_m \\ o_1 & L_2'(\tau) & \cdots & o_m \\ \vdots & \vdots & \ddots & \vdots \\ o_1 & o_2 & \cdots & L_m'(\tau) \end{bmatrix} \Omega^{-1}\Psi \\ &\triangleq \begin{bmatrix} K_{xs} & K_{ys} \end{bmatrix} \quad (54) \end{aligned}$$

Similarly, we can get u_f using MPC for the fast subsystem. Then composite input $u(t)$ for the original system is obtained:

$$u = u_s + u_f \quad (55)$$

Then, we can get the model predictive control for the original system in the same way.

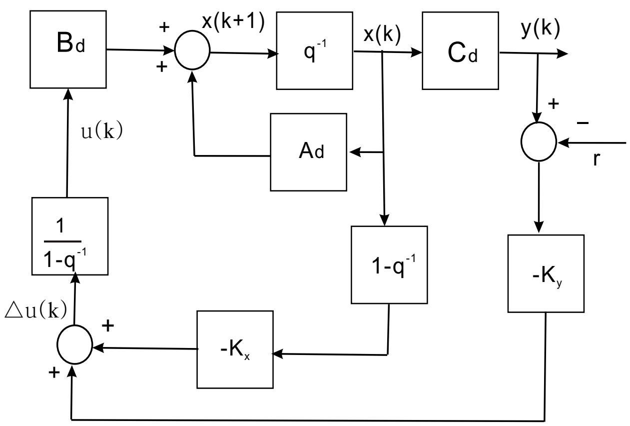

Figure 4: Block diagram of Discrete-Time MPC Method

4.2 Discrete-Time Model Predictive Control

Here we provide the discrete-time model predictive control method to compare with the continuous-time model predictive control.

Fig. 4 is the closed-loop block diagram of discrete-time MPC method from [12], where q^{-1} denotes the backward shift operator. The diagram shows the state feedback structure for the discrete-time model predictive control (DMPC) with integral action in which the module $\frac{1}{1-q^{-1}}$ denotes the discrete-time integrator.

Consider a discrete-time system as below:

$$\begin{aligned} x(k+1) &= A_d x(k) + B_d u(k); && (56) \\ y(k) &= C_d x(k) && (57) \end{aligned}$$

where u is the input variable; y is the process output, and $x(k)$ is the state variable vector with assumed dimension n.

We define

$$\begin{aligned} \triangle x(k+1) &= x(k+1) - x(k) && (58) \\ &= A_d(x(k) - x(k-1)) \\ &\quad + B_d(u(k) - u(k-1)) \\ \triangle u(k) &= u(k) - u(k-1) && (59) \end{aligned}$$

Then easily we can obtain the augmented model as below from equation (56-57),

$$\overbrace{\begin{bmatrix} \triangle x(k+1) \\ y(k+1) \end{bmatrix}}^{X_d(k+1)} = \overbrace{\begin{bmatrix} A_d & 0' \\ C_d A_d & 1 \end{bmatrix}}^{\widetilde{A}_d} \overbrace{\begin{bmatrix} \triangle x(k) \\ y(k) \end{bmatrix}}^{X_d(k)} + \underbrace{\begin{bmatrix} B_d \\ C_d B_d \end{bmatrix}}_{\widetilde{B}_d} \triangle u(k), \qquad (60)$$

$$y(k) = \overbrace{\begin{bmatrix} 0 & I \end{bmatrix}}^{\widetilde{C}_d} \begin{bmatrix} \triangle x(k) \\ y(k) \end{bmatrix} \qquad (61)$$

Note N_c as the control horizon dictating the number of parameters used to capture the future control trajectory.

Our aim is to find the best control parameter vector $\triangle U$=$[\triangle u(k_i)\ \triangle u(k_i+1)\ \cdots\ u(k_i+N_c-1)]$ such that the error between the set-point signal and the predicted output signal is minimized.

Define the cost function J that reflects the control objective as

$$J = (R_s - Y)' Q_d (R_s - Y) + \triangle U' R_d \triangle U \qquad (62)$$

where N_p is the length of the optimization window; $Q_d \geq 0$ and $R > 0$ are weighting matrices with appropriate dimensions; Y is the vector of predicted output variables defined as

$$Y = [y(k_i+1|k_i)\ y(k_i+2|k_i)\ \cdots\ y(k_i+N_p|k_i)]'$$

and $R_s' = \overbrace{\begin{bmatrix} 1 & 1 & \cdots & 1 \end{bmatrix}}^{N_p} r(k_i)$ is the reference signal;

At time k_i, the control trajectory $\triangle u(k_i)$, $\triangle u(k_i+1), \cdots, \triangle u(k_i+N_c-1)$ is regarded as the impulse response of a stable dynamic system, Thus, a set of discrete-time Laguerre functions $L(k) = [l_1(k)\ l_2(k)\ \cdots\ l_N(k)]'$ which are generated from the discretization of continuous-time Laguerre functions are used to describe the difference of the control variable

$$\triangle u(k_i+k) = \sum_{j=1}^{N} c_j(k_i) l_j(k) = L(k)' \eta_d \qquad (63)$$

with k_i being the initial time of the moving horizon window and k being the future sampling instant; N is the number of terms used in the expansion and $c_j,\ j = 1, 2, \cdots, N$, are the coefficients, and they are functions of the initial time of the moving horizon window k_i, and $\eta = [c_1\ c_2 \cdots c_N]'$ is the vector of coefficients.

Using the partial derivative of the cost function, we can obtain the minimum value of the cost function J_{min} is

$$J_{min} = X_d(k_i)' \left(\sum_{m=1}^{N_p} (\widetilde{A}_d')^m Q_d (\widetilde{A}_d)^m - \Psi_d' \Omega_d^{-1} \Psi_d \right) X_d(k_i) \qquad (64)$$

where

$$\Phi_d(m)' = \sum_{i=0}^{m-1} \widetilde{A}_d^{m-i-1} \widetilde{B}_d L'(i) \quad (65)$$

$$\Omega_d = \sum_{m=1}^{N_p} \Phi_d(m) Q_d \Phi_d'(m) + R_L \quad (66)$$

$$\Psi_d = \sum_{m=1}^{N_p} \Phi_d(m) Q_d A_d^m \quad (67)$$

leading to

$$\eta_d = -\Omega_d^{-1} \Psi_d X_d(k_i) \quad (68)$$

Thus the control $\triangle u(k)$ can be written in the form of linear state feedback control by replacing k_i with k. Namely,

$$\begin{aligned} \triangle u(k) &= -L(0)\Omega_d^{-1}\Psi_d X_d(k_i) \\ &= -K_{dmpc} X_d(k_i) \end{aligned} \quad (69)$$

And the feedback gain matrix is as below:

$$K_{dmpc} = L(0)\Omega_d^{-1}\Psi_d \quad (70)$$

5 Simulation Results

Both Continuous-Time (CT) MPC controllers for the high-order (original) and low-order (decoupled) wind energy conversion systems were obtained using MATLAB®[1].

Also Discrete-Time (DT) MPC controller is designed using the discretized wind energy conversion system with sample interval, $T_s = 0.1s$.

All reference signals are set zeros. Output coefficients are chosen as:

$$C_f = \begin{bmatrix} 1 & 0 \\ 0 & 1 \end{bmatrix}, C_s = \begin{bmatrix} 1 & 1 & 1 \end{bmatrix},$$
$$C = \begin{bmatrix} 1 & 0 & 0 & 0 & 0 \end{bmatrix}$$

Weighting matrices Q, R, Q_s, R_s, Q_f, and R_f were chosen as below:

$$\begin{aligned} Q &= C'C, \quad Q_s = C_s'C_s, \quad Q_f = C_f'C_f, \\ R &= R_s = R_f = 0.2 \times I_{3\times3} \end{aligned}$$

The simulation results are depicted in Fig. (5-9).

From Fig. 5-6 and Fig. 8-9, we can tell the responses of high-order and low-order model predictive controllers of the states ω_r, ω_g, i_d and i_q are very close. And for the state T_h in Fig. 7, the convergence of the low-order model predictive controller is quicker and more accurate than that of the high-order model predictive controller. It proves that the composite model predictive controller gives more accurate results than the model predictive control of the original system with less computation effort. In addition, the performance of discrete-time model predictive controller converges much quicker than that of the continuous-time model predictive controllers.

[1]MATLAB is registered trademarks of The Mathworks, Inc., Natick, MA, USA.

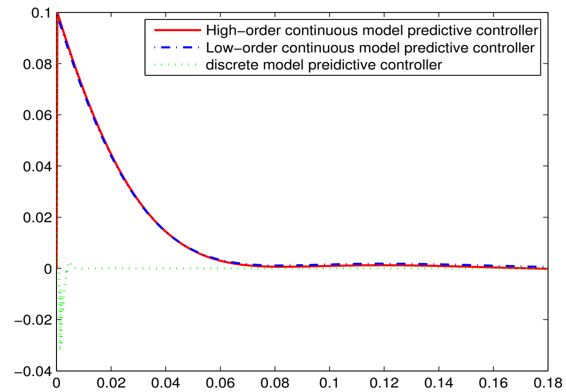

Figure 5: The state ω_r response of the high-order and low-order CT model predictive controllers and DT model predictive controller

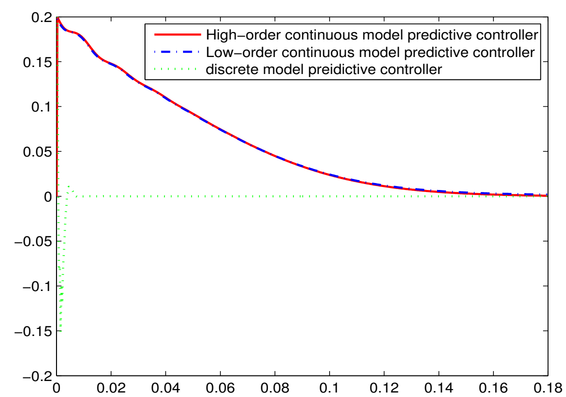

Figure 6: The state ω_g response of the high-order and low-order CT model predictive controllers and DT model predictive controller

6 Conclusion

This paper presents time scale analysis and synthesis (control) methodology for continuous-time Model Predictive Control (MPC). In this method, a higher-order plant, wind energy conversion system, with a

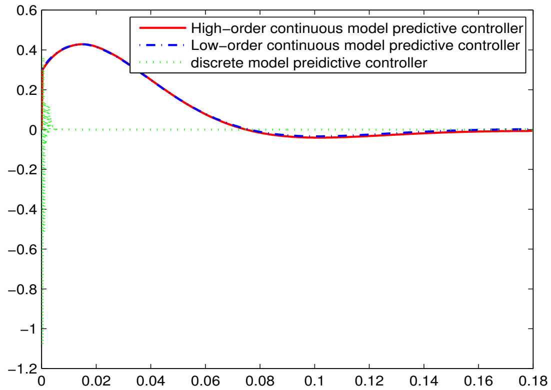

Figure 7: The state T_h response of the high-order and low-order CT model predictive controllers and DT model predictive controller

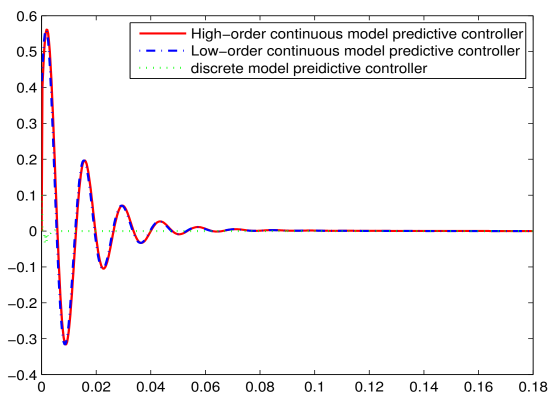

Figure 8: The state i_d response of the high-order and low-order CT model predictive controllers and DT model predictive controller

two-time-scale (slow and fast) character is decoupled into low-order slow and fast subsystems and sub-augmented systems. Then slow and fast sub-controllers based on continuous-time MPC method are synthesized (designed) separately and a composite MPC is obtained. Then discrete-time MPC is introduced comparing with the continuous-time MPC. The results show that the performance of the system with continuous-time composite MPC is more accurate than that of the continuous-time MPC of the original high-order system with simpler design and reduced computational effort. The performance of discrete-time model predictive controller converges much quicker than that of the continuous-time model predictive controllers.

Acknowledgements: The research is supported jointly by the China Scholarship Council and the National Natural Science Foundation of P. R. China under Grant 61104064, 61174038 and conducted at the Measurement and Control Engineering Research Center at Idaho State University, USA.

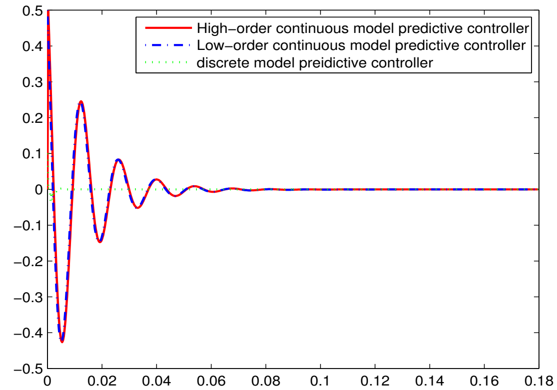

Figure 9: The state i_q response of the high-order and low-order CT model predictive controllers and DT model predictive controller

References:

[1] D.S. Naidu, Singular Perturbations and Time Scales in Control Theory and Application s: an Overview, *Dynamics of Continuous, Discrete and Impulsive Systems Series B: Applications and Algorithms* 9, 2002, pp. 233–278.

[2] Bahador Makki and Baharak Makki, Control Design for Uncertain Singularly Perturbation Systems with Discrete Time Delay, *WSEAS Transactions on Systems and Control* 6, Dec. 2011, pp. 456-465, .

[3] H.M. Nguyen and D.S. Naidu, Time Scale Analysis and Control of Wind Energy Conversion Systems, *2012 5th International Symposium on Resilient Control Systems (ISRCS)*, 2012, pp. 149–154.

[4] Yingchen Xue and Nengling Tai, System frequency regulation investigation in doubly fed induction generator (DFIG), *WSEAS Transactions on Power Systems* 7, Jan. 2012, pp. 18-26.

[5] M. Stiebler, *Wind Energy Systems for Electric Power Generation*, Springer-Verlag, 2008.

[6] P. Musgrove, *Wind Power*, Cambridge University Press, 2010.

[7] H.J. Wagner and J. Mathur, *Introduction to Wind Energy Systems: Basics, Technology and Operation*, Springer-Verlag, Berlin Heidelberg, 2009.

[8] D.A. Spera, *Wind Turbine Technology: Fundamental Concepts of Wind Turbine Engineering, 2nd Edition*, ASME Press, 2009.

[9] H. M. Nguyen and D. S. Naidu, Singular Perturbation Analysis and Synthesis of Wind Energy Conversion Systems under Stochastic Environments, *Proceedings of the 12th WSEAS International Conference on Advances in Systems Theory, Signal Processing and Computational Science*,Istanbul, Turkey, August 21-23, 2012, pp. 283-288.

[10] D.S. Naidu, *Singular Perturbation Methodology in Control Systems*, Peter Peregrinus Ltd., 1988

[11] D. Q. Mayne, J. B. Rawlings, C. V. Rao and P. O. M. Scokaert, Constrained model predictive control: Stability and optimality, *Automatica* 36, 2000, pp. 789-814.

[12] L. Wang, *Model Predictive Control System Design and Implementation Using MATLAB",* Springer, 2009

[13] C. E. Garcia and D. M. Prett and M. Morari, Model predictive control: theory and practice - a survey, *Automatica* 25, 1989, pp. 335–348.

[14] M. Morari and J. H. Lee, Model predictive control: past, present and future, *Computers and Chemical Engineering*, 1999, pp. 667-682.

[15] X. Chen and M. Heidarinejad and J. Liu and P. D. Christofides, Composite fast-slow MPC design for nonlinear singularly perturbed systems: Stability analysis, *American Control Conference (ACC)*, 2012, pp. 4136 –4141.

[16] J. Niu and J. Zhao and Z. Xu and J. Qian, A Two-Time Scale Decentralized Model Predictive Controller Based on Input and Out put Model, *Hindawi Publishing Corporation Journal of Automated Methods and Management in Chemistry*, 2009, pp. 1–11.

[17] Nikos E. Mastorakis, Cornelia Aida Bulucea, Gheorghe Manolea, Marius Constantin Popescu, and Liliana Perescu-Popescu, Model for Predictive Control of Temperature in Oil-filled Transformers, *Proceedings of the 11th WSEAS International Conference on Automatic Control, Modelling and Simulation*, 2009, pp. 157-165.

[18] H. Li and Z. Chen, Overview of different wind generator systems and their comparisons, *IET Renewable Power Generation* 2, Jun. 2008, pp. 123 C138.

[19] K.W. Chang, Non–stationary flows of viscous and ideal fluids in $\mathbb{R}^3$, *SIAM Journal of Mathematical Analysis* 3, 1972, pp. 520–526.

[20] T. Grodt and Z. Gajic, The recursive reduced-order numerical solution of the singularly perturbed matrix differential Riccati equation, *IEEE Transactions on Automatic Control* 34, 1988, pp. 751–754.